

Distinct Fault Analysis of Induction Motor Bearing using Frequency Spectrum Determination and Support Vector Machine

Shrinathan Esakimuthu
Pandarakone

Student Member, IEEE
Nagoya Institute of Technology
Gokiso-cho, Showa-ku
Nagoya, 466-8555, Japan
sarushrinathan@gmail.com

Yukio Mizuno

Member, IEEE
Nagoya Institute of Technology
Gokiso-cho, Showa-ku
Nagoya, 466-8555, Japan
mizuno.yukio@nitech.ac.jp

Hisahide Nakamura

Member, IEEE
TOENEC Corporation
1-79, Takiharu-cho, Minami-ku,
Nagoya, 457-0819, Japan
hisahide-nakamura@toenec.co.jp

Abstract – In modern industrial environment, the demand for the condition monitoring and the maintenance management for the induction motor has been increased. Among all the components of the induction motor, bearing is the critical component and the fault occurring in it has to be considered as a major issue. Usually, the bearing fault can be detected by the vibrational analysis. However, this method has a disadvantage that location of the equipment is not always easily accessible and also quite costly. Thus, in this paper, the experiment for detecting the fault in the bearing of the three phase induction motor is achieved by the frequency selection in the stator current spectrum. Their feature was evaluated by Fast Fourier Transform and the diagnosis was performed by Support Vector Machine. Experimental results were obtained, considering two types of outer raceway bearing faults at different load conditions and the promising results were obtained.

Index Terms—Spectral analysis, induction motor, bearing damage, condition monitoring, stator current, fault diagnosis, Support Vector Machine.

I. INTRODUCTION

Having various advantages like easy handling, low cost, high reliability, high efficiency, robustness and the availability of the power converters makes the induction motor as most suited for the industrial applications. In many industries, however, the induction motor is being operated without proper maintenance and condition monitoring. When we visualise from the economical point of view, maintaining the induction motor properly and replacing the faulty motor is quite cheaper, rather than letting the faulty motor to shut down the entire company. Therefore, proper maintenance and condition monitoring is adequate to make the motor sustainable for a longer duration.

For the last couple of decades, numerous technique has been developed for identifying the fault in the electrical machinery and many types of researchers are still undergoing. Among all the mechanical failure, bearing faults are the most common faults in an electric motor followed by the stator faults and rotor faults according to the induction motor reliability study [1]-[3]. These bearing failure may cause the industry to shut down, loss of production and even it may create an origin for

catastrophic effect and human casualties [4]-[5]. The detection of the bearing fault at the incipient stage will avoid the unexpected breakdown and automatically increase the reliability of operation [6]-[8].

Most of the research for detecting the bearing failure is done based on the vibration analysis [9]-[11]. Although this method is quite effective, the analysis will vary based on the location of the equipment and so it is difficult for choice and positioning of the sensor. In order to overcome the disadvantage of the above method, detection is done by means of the stator current [12]-[14] so that choice and positioning of the sensor are not required. Some of the other bearing fault detection methods are based on time domain analysis [15]-[17] and electric current analysis [18]-[21]. Both the analysis produced promising results and gained prominence.

In most of the cases, the artificial bearing fault was introduced as hole [20], [22]-[24]. In order to explain the objective of this paper, a short overview of the result is discussed. As a case, Valeria *et al.* [22] carried out the experiment for the hole of diameter 2.3 mm and 2.8 mm and able to distinguish the healthy motor and faulty motor. The detection of bearing fault is achieved by spectral kurtosis and envelope analysis of stator current. However, no results were obtained regarding the smaller size of the hole. Also, Christelle and Kay Hameyer [23] carried out the diagnosis for two lower level width of the hole. The fault examination and diagnosis are carried out by means of the linear discriminant analysis of stator current features from the selected frequency components. Although the faulty motors are distinguished from the healthy motors, the difference between the two types of fault cannot be observed by this method.

The authors have carried out researches to establish a simple and reliable diagnosis method for broken rotor bar and bearing of a cage induction motor based on the load current [25]. In this previous paper, it was found that the method is suitable for broken rotor bar as well as for identifying even a slight mechanical failure. That is, both the classification and specification of number of rotor bar can be achieved by this method. However, authors have done partial investigation in

diagnosing the fault occurred in bearing of induction motor.

Thus, the objective of the present paper is to establish a method to diagnose not only the difference between the healthy motor and faulty motor, but also the difference between two types of faulty motor by considering the rotating speed of the induction motor. Analysis is carried out by characterising the frequency spectrum of the load current and to be considered as the main feature. In order to enhance the accuracy of the proposed method, a novel diagnostic method is proposed with the help of Support Vector Machine (SVM).

This paper is organised as follows: Section II gives a brief description of the types of bearing damage and the analytical calculation of the outer raceways effects. In section III, the experimental setup and types of bearing faults used in the present study are discussed. Section IV describes the FFT analysis and the feature extraction. Section V presents the SVM diagnosis method. Finally, the conclusion and the future task is discussed in section VI.

II. LOCALIZATION OF BEARING FAULTS

In general, bearing faults can be categorized as two types. They are distributed faults and localized faults [26]. Among the two types of faults, distributed faults can affect the whole current spectrum and it is highly difficult to characterize them based on the distinct frequencies. On the other hand, localized faults can be easily characterized. Normally, single-point defects are localized faults and that can be easily classified according to their affected element [18]. In fact, many research works have been focusing on the single-point defects [27]-[29]. In contrast, single-point localized defects can be classified as the following: outer raceway defects, inner raceway defects, ball defects and cage defect.

Normally, the bearing consists of outer and inner raceway, and both these raceways are separated by the rolling elements like balls or cylindrical rollers. Suppose, if a damage occurs in the bearing, then there is a possibility for shock pulses with characteristics frequencies to occur. This incident happens when the ball or rolling element passes through the damaged portion. Mainly, characteristic frequency components depend on the damaged part of the bearing and we are able to calculate them by means of the geometry of the rolling elements and the mechanical rotating frequency f_r . A detailed calculation of these analysis can be found in [30].

Among the single-point localized defects, outer raceway defects is discussed in this paper. The characteristic frequency takes the following expression.

$$f_o = \frac{N_b}{2} f_r \left(1 - \frac{D_b}{D_c} \cos \beta \right) \quad (1)$$

Also, it has been statically shown in [31], that the characteristic frequency can be approximated by the number of roller bearing between 6 and 12. It takes the following expression.

$$f_o = 0.4 N_b f_r \quad (2)$$

Where N_b is the number of balls or bearing rollers, β is the contact angle between the ball and raceway, D_b is the diameter of the ball or bearing roller, D_c is the diameter of the cage.

TABLE I
DATA OF THE BEARING

Bearing specification	Dimension
Inner diameter d	25mm
Outer diameter D	52 mm
Roller diameter D_b	13.5 mm
Cage diameter D_c	38.5mm
Number of balls N_b	9

In the present study, cylindrical roller bearing is used and the hole is created by drilling the outer raceway. The characteristic fault frequency for the outer raceway defects is calculated based on the geometric specification of the bearing as illustrated in TABLE I. According to [4], the contact angle is 0° for the case of cylindrical roller bearing. Therefore, based on the specified values of the bearing, the characteristics frequencies from the equation (1) and (2) attains the value of 87.5 Hz and 108 Hz. The mechanical rotating frequency f_r of induction motor is 30Hz.

III. EXPERIMENTAL SETUP AND FAULT DESCRIPTION

Fig. 1 shows the experimental setup to record the current and voltage waveform for detecting the bearing fault. Using the current probes (HIOKI 9696-02) and voltage probes (HIOKI 9666), both the current and voltage were measured at the given rotating speed. Also, the rotating speed was monitored with a speed indicator (ONOSOKKI HT-5500). Outputs from the sensor were recorded simultaneously with the measurement system developed by the authors. Also, the various output signal from the different sensors was transferred to the PC through the measurement equipment and are recorded. This measurement equipment has eight BNC input terminals and A/D converters. The sampling time is set to 10 μ s and the data recording length is 2^{17} per channel. Also, the frequency resolution is 0.76 Hz. In the prompt study, 7 channels (3 current, 3 voltage and rotating speed) were used. The data acquisition was triggered for every 30 s by a timer and it should be noted that the time required for the data transfer of 7 channels was less than 20 s.

A three phase induction motor (2.2 kW, 200 V, 8.5 A, 1740 min^{-1}) was used as a specimen. The stator winding is a double star connection. Typically, it is tedious and costly work to collect the motors with the damage in the bearing, which occurred during the operation at the site. Due to this reason, in the present study, a two type of artificial faults was introduced to the outer raceway of the bearing in the induction motor. Three types of bearing conditions are discussed: one healthy and two bearings with the artificially made holes. The details about the specification of the hole are listed in TABLE II. The healthy motor was tested for reference under the same condition before the artificial hole was made.

The bearing with two types of artificial fault is shown in Fig. 2. Also, the procedure of analysis for diagnosing the bearing

fault is shown in Fig. 3. The experimental work begins with the observation made in the healthy motor. After that, the healthy bearing was replaced with the faulty bearing

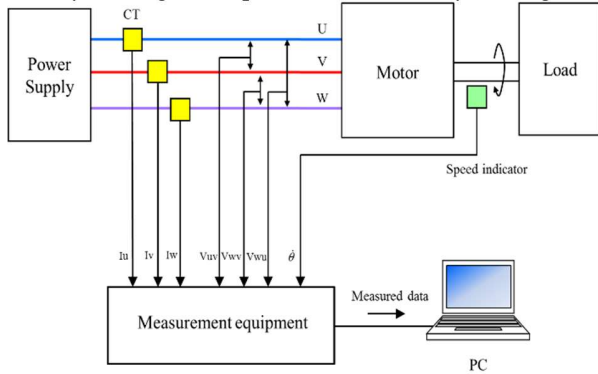


Fig. 1. Experimental Setup.

TABLE II
HOLE SPECIFICATION

Fault type	Diameter (mm)	Depth (mm)
F1	0.5	1
F2	2	1

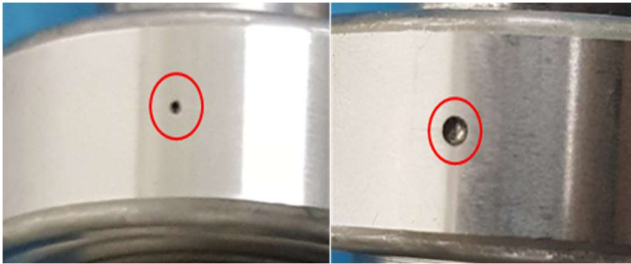


Fig. 2. Bearing with a hole 0.5 mm (left) and hole 2 mm (right).

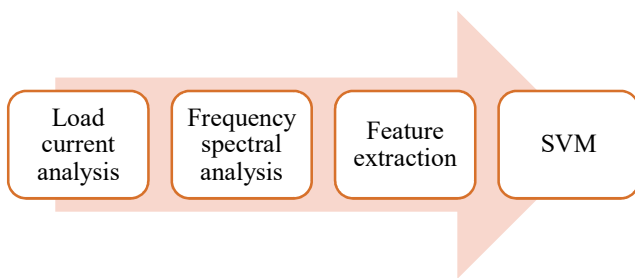


Fig. 3. Analysis Procedure.

of hole 0.5 mm and performed the same analysis which has been carried out for the healthy bearing. Later, once again the experiment was carried out by changing the dimension of the hole in the bearing to 2 mm and the same analysis was performed. The rotating speed was adjusted from 1780 min^{-1} to 1765 min^{-1} .

For easy understanding of analysis, the following description will be applied in this paper: HF1: Comparison between the healthy motor and fault motor with the bearing hole of 0.5 mm. HF2: Comparison between the healthy motor

and faulty motor with the bearing hole of 2 mm. F1F2: Comparison between the two faulty motors with the bearing hole of 0.5 mm and 2 mm. HF1F2: Comparison between the healthy motor and faulty motors with bearing hole of 0.5 mm and 2 mm. Totally four analysis has been made in this paper.

IV. INVESTIGATION ON FREQUENCY SPECTRAL ANALYSIS AND FEATURE EXTRACTION OF LOAD CURRENT

The proposed method is evaluated by means of measuring the stator current. The current signals are collected from the healthy motor and two types of the faulty motors under various rotating speed. The measurement was carried out under the load condition. Both the frequency spectrum analysis and the feature extraction are based on the value of the stator current under three types of bearing conditions.

A. Frequency Spectral Analysis

FFT analysis of the U-phase load currents was performed for all the three types of bearing conditions. For the clear view of explanation, 1780 min^{-1} rotating speed is selected. The compared frequency spectrum of the load current at the given condition HF1, HF2, F1F2 and HF1F2 are shown from Fig. 4 to Fig. 7, respectively. The amplitude of the vertical axis is normalized so that the maximum level of frequency spectrum to be 0 dB. The frequency of the power source is 60 Hz. This condition is common for all the four analysis.

At the frequency of 87.5 Hz and 108 Hz, the difference in the amplitude of the frequency components was not observed. Due to this reason, for all the four analysis (HF1, HF2, F1F2 and HF1F2), the amplitude difference of the frequency component is observed at the frequency of 30 Hz and 90 Hz with respect to other frequencies. There is a reason why the amplitude difference is observed at the frequency components of 30 Hz and 90 Hz. The explanation will be illustrated as follows:

In general, in the case of 4 pole induction motor, the synchronous speed N_s is 1800 min^{-1} . By this it is clear that, the motor rotates at 30 revolutions per second and the concerned frequency is 30 Hz. On overview, both the frequency 30 Hz and 90 Hz is not included in the power supply voltage (60 Hz). However, the current flowing in the motor is affected by two components: rotating speed and the two signal (30 Hz and 90 Hz) that appears in the spectrum of the current as a sideband of fundamental frequency component of the supplied voltage. As an illustration, for the case of 1780 min^{-1} , the motor rotates at $1780/60$ (revolutions/sec) and it takes a value of 29.67 Hz. In general, when the motor rotates at 1780 min^{-1} , two signals will be appeared in the spectrum of the current. They are 30.33 Hz ($60\text{Hz}-29.67\text{Hz}$) and 89.67 Hz ($60\text{Hz}+29.67\text{Hz}$).

Also, it is evidently known fact that frequency of the current spectrum will change according to rotating speed. But still for other three rotating speed (1775 min^{-1} , 1770 min^{-1} and 1765 min^{-1}), the changes in the amplitude of load current is observed at the same frequency level 30 Hz and 90 Hz. This is due to the frequency resolution of the measured equipment involved in the proposed system is 0.76 Hz. As a result of low frequency resolution, it is highly impossible to discriminate the changes

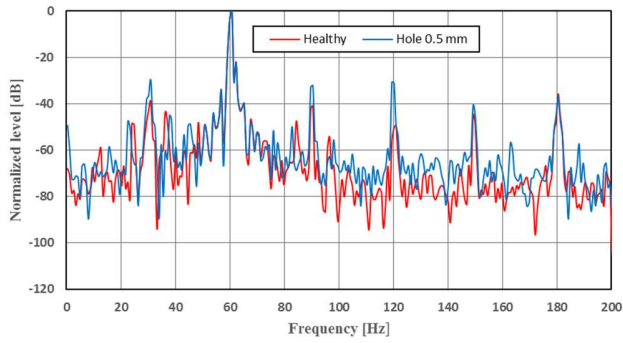


Fig. 4. Spectral analysis for HF1 at 1780 min⁻¹.

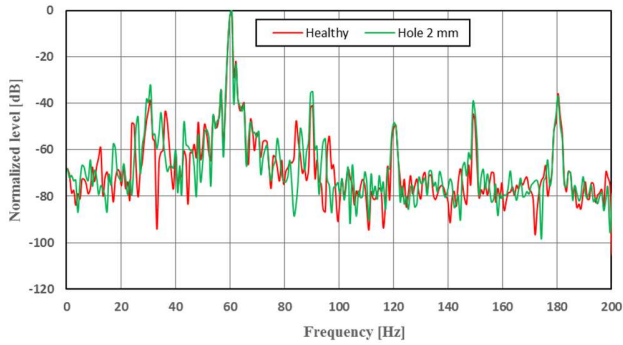


Fig. 5. Spectral analysis for HF2 at 1780 min⁻¹.

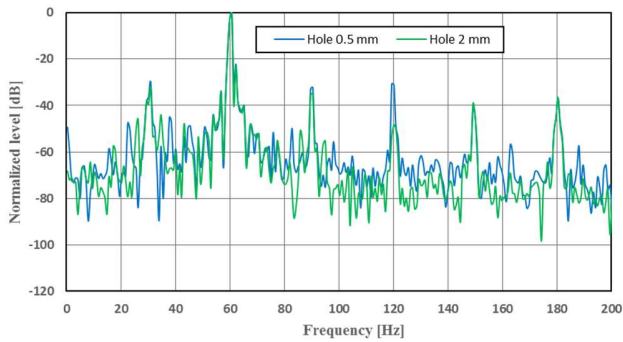


Fig. 6. Spectral analysis for F1F2 at 1780 min⁻¹.

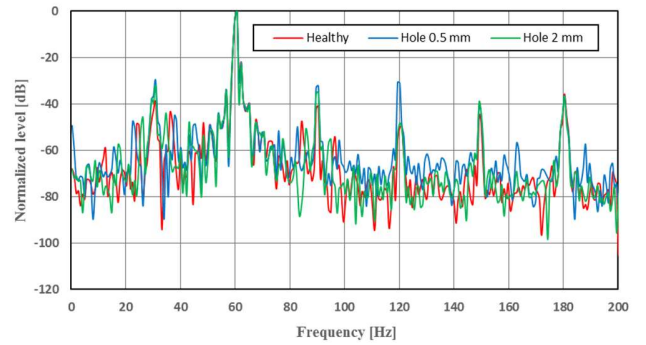


Fig. 7. Spectral analysis for HF1F2 at 1780 min⁻¹.

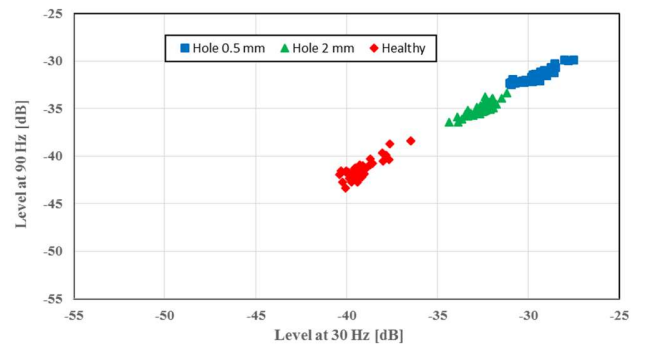


Fig. 8. Feature distribution at 1780 min⁻¹.

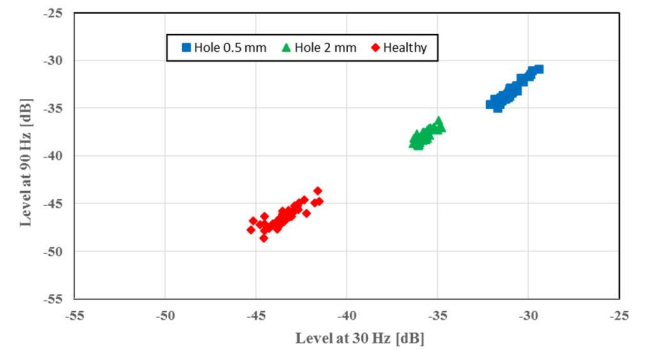


Fig. 9. Feature distribution at 1775 min⁻¹.

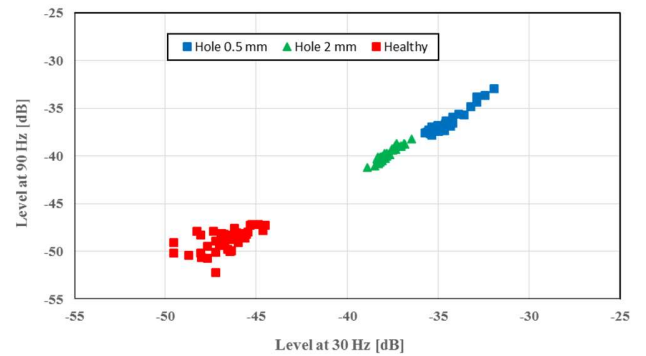


Fig. 10. Feature distribution at 1770 min⁻¹.

that will happen in the frequency of current spectrum features. Thus the frequency component 30 Hz and 90 Hz plays an important role in scrutiny the spectral analysis.

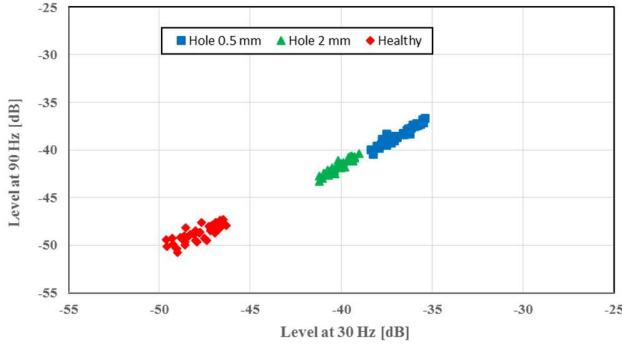


Fig. 11. Feature distribution at 1765 min⁻¹.

As a result of a change in the amplitude of the frequency component, the authors can distinguish both the healthy motor and faulty motor, irrespective of the bearing condition. The key point to be noted is that it is not only the healthy motor gets differentiated from the faulty motor, but also the authors are able to distinguish the two types of faulty motor. The change in the amplitude of the frequency component between the two types of bearing condition (Hole of 0.5 mm and 2 mm) is observed. Therefore, these levels are considered as one of the significant features in the present study.

B. Feature Extraction

For both healthy motor and faulty motors, the contribution of each feature is evaluated for all the considered load condition. Feature distribution at the frequency level of 30 Hz and 90 Hz for all the three types of bearing condition with respect to rotating speed (1780 min⁻¹, 1775 min⁻¹, 1770 min⁻¹ and 1765 min⁻¹) is shown from Fig. 8 to Fig. 11. These features obtained under the given condition gather closely to each other and are distributed in a limited class. The location of the distributed class depends on the rotating speed and the bearing condition.

It is clear that, while taking the individual rotating speed of the induction motor into consideration, the class of the faulty motor (Hole of 0.5 mm and 2 mm) is located far away from the healthy motor. Another interesting point to be considered is the class of the faulty motor with a hole of 0.5 mm located apart from the faulty motor with the hole of 2 mm. Both these holes has the own class of location according to the bearing condition and rotating speed. Thus, this method is effective in diagnosing the three types of bearing condition.

V. DIAGNOSIS VIA SUPPORT VECTOR MACHINE

In this section, diagnosis is performed with the help of Support Vector Machine and the accuracy of the result is discussed.

A. Explanation of SVM

SVM is used as a tool for the diagnosis in the present study. Its concept is described shortly. SVM is one of the diagnosing tools which determines recognition results by categories, and that can be attained after evaluating similarities of an input pattern with respect to categories, on the basis of the previous

recognition results of training data [32]. This SVM was originally introduced to the classification of linear classes of objects. In addition to performing linear classification, it can efficiently perform a non-linear classification using the kernel, implicitly mapping their inputs into high-dimensional feature spaces.

In this present study, Soft Margin SVM was applied to a two or three-class model of an induction motor in order to diagnose the mechanical failure. R language was used as a programming tool. In Soft Margin SVM, we have two important parameters: cost parameter C and gamma parameter γ . Generally the cost parameter C is introduced to control the trade-off between maximizing the margin and minimizing the training error. On further, Radial Basis Function kernel is used, which is a commonly used as a kernel function in support vector. Mainly, the definition of the kernel involves gamma parameter γ .

In addition, both the tuning of parameters C and γ were carried out by 8-cross-validation. Initially, the data was divided into 8 groups. The data's from Groups 1 to 7 were used for training data. And finally the data from Group 8 was used for evaluation data. Evaluation data is used for obtaining the diagnosis accuracy rate. Then, by changing the group alternatively for evaluation, 7 successive accuracy rates were obtained. Finally, the average accuracy rate was calculated. The above said process was repeated for different values of C and γ . As a result, the value 1.0 and 0.333 were adopted for C and γ , respectively. Obtaining the optimum parameter values will be a tedious process, however the process that we have followed would be practically acceptable.

B. Diagnosis Procedure

Diagnosis based on the SVM was performed. This diagnosis is carried out by considering the individual rotating speed of the induction motor for all the three types of bearing condition. Specifically, the analysis is done on the three types of bearing condition with respect to rotating speed. As an illustration, for the case of single rotating speed, around 80 sets of load current data were obtained for the condition HF1, HF2 and F1F2. Each data consists of two components that are the amplitude of frequency components at 30 Hz and 90 Hz. Among the 80 sets of load current data, 60 data were used as a training data and the remaining 20 data were used as a verification data. Similarly, for the case of HF1F2, among the 120 sets of load current data, 90 data were used as a training data and the remaining 30 data were used as diagnosis data. With respect to bearing condition (HF1, HF2, F1F2 and HF1F2), the diagnosis was performed by using SVM for all rotating speed (1780 min⁻¹, 1775 min⁻¹, 1770 min⁻¹ and 1765 min⁻¹). In this paper, the accuracy rate of the diagnosis is defined as

$$\text{accuracy rate (\%)} = \frac{\text{number of data diagnosed accurately}}{\text{total number of data for diagnosis}} \times 100 \quad (3)$$

Based on the above mentioned formula, in the present analysis, the diagnosis is performed under two trials, trial I and trial II.

C. Trial I

In the case of the trial I, for single rotating speed, among the 40 verification data, first 30 data have been taken as the training data and the rest 10 data as diagnosis data. Likewise, the process is done for all rotating speed (1780 min^{-1} , 1775 min^{-1} , 1770 min^{-1} and 1765 min^{-1}). The above mentioned condition will be applied to the four types of bearing analysis (HF1, HF2, F1F2 and HF1F2) and the trial I is performed. The accuracy rate of diagnosis for the cases HF1, HF2, F1F2 and HF1F2 with respect to 1780 min^{-1} rotating speed is shown from TABLE III to TABLE VI, respectively.

A yellow-colored cell reveals the case where the proper diagnosis is performed. The level of accuracy rate for all the rotating speed concerning the four types of bearing analysis is discussed below.

TABLE III
TRIAL I DIAGNOSIS RESULT OF HF1 at 1780 min^{-1}

		Bearing condition of target motor	
		Healthy	Hole 0.5 mm
Results of diagnosis	Healthy	10	0
	Hole 0.5 mm	0	10
Accuracy rate (%)		100	100
Total accuracy rate (%)		100	

TABLE IV
TRIAL I DIAGNOSIS RESULT OF HF2 at 1780 min^{-1}

		Bearing condition of target motor	
		Healthy	Hole 2 mm
Results of diagnosis	Healthy	10	0
	Hole 2 mm	0	10
Accuracy rate (%)		100	100
Total accuracy rate (%)		100	

TABLE V
TRIAL I DIAGNOSIS RESULT OF F1F2 at 1780 min^{-1}

		Bearing condition of target motor	
		Hole 0.5 mm	Hole 2 mm
Results of diagnosis	Hole 0.5 mm	10	0
	Hole 2 mm	0	10
Accuracy rate (%)		100	100
Total accuracy rate (%)		100	

TABLE VI
TRIAL I DIAGNOSIS RESULT OF HF1F2 at 1780 min^{-1}

		Bearing condition of target motor		
		Healthy	Hole 0.5 mm	Hole 2 mm
Results of diagnosis	Healthy	10	0	0
	Hole 0.5 mm	0	10	1
	Hole 2 mm	0	0	9
Accuracy rate (%)		100	100	90
Total accuracy rate (%)		96.67		

1) 1780 min^{-1} :

The bearing fault investigation was initially started with the 1780 min^{-1} rotating speed. As a result of diagnosis, total accuracy rate for HF1, HF2 and F1F2 is 100 %. But for the case of HF1F2, the total accuracy rate is slightly decreased to 96.67 %. It is very clear from the diagnosis result that the high accuracy rate is achieved even for the slight mechanical failure in the bearing of the induction motor.

2) 1775 min^{-1} , 1770 min^{-1} and 1765 min^{-1} :

The next step of bearing examination is done for the other rotating speed. This subsidiary is dealing with the 1775 min^{-1} , 1770 min^{-1} and 1765 min^{-1} rotating speed and its diagnosis results were discussed. For all the four cases of bearing analysis (HF1, HF2, F1F2 and HF1F2), the total accuracy rate of diagnosis is 100 %. This result is similar for all the rotating speed cited in this sub-section.

In addition to above description and for the sake of clear understanding, Fig. 12 is plotted. This fig shows the entire combination of the four type of bearing analysis, having rotating speed plotted against the x-axis and accuracy level against the y-axis. From the Fig. 12, it is evidently proved that the proper diagnosis can be done for all the three types of bearing condition by considering the rotating speed of the induction motor. Also the Fig. 12 shows the accuracy level for both the individual rotating speed as well as for the combined data of all the rotating speed that is carried out for all the four types of bearing analysis HF1, HF2, F1F2 and HF1F2, respectively.

D. Trial II

Trial II is followed by trial I. This trial II is mainly done to evaluate the accuracy level of diagnosis and also for the quality assurance of the proposed method. In this trial II, for the case of single rotating speed 1780 min^{-1} , among the 40 verification data, first 10 data has been taken as the diagnosis data and the rest 30 data as training data. This system is completely a reverse order of trial I. Similarly, it is done for the other rotating speed as well (1780 min^{-1} , 1775 min^{-1} , 1770 min^{-1} and 1765 min^{-1}).

The above mentioned plight will be applied to all the three types of bearing condition and the trial II is performed to the four types of bearing analysis (HF1, HF2, F1F2 and HF1F2). The diagnosis rate for the cases HF1, HF2, F1F2 and HF1F2 is 100 %. This result is same for all the rotating speed and it is openly seeable from the Fig. 13. Thus the proposed system and the level of diagnosis rate is practically acceptable by considering the rotating speed of the induction motor.

E. Further Discussion

Thus both the trial I and trial II is performed by considering the rotating speed of the induction motor for all the four cases of analysis (HF1, HF2, F1F2 and HF1F2). The overall average accuracy rate for trial I and trial II is given as 99.17 % and 100 %, respectively. Thus, it is very clear that difference in the accuracy level between the trial I and trial II is negligible.

Almost, the accuracy rate and the total accuracy rate is same in both the trial I and trial II. Till now the discussion is done by considering the rotating speed of the induction motor.

In further, the diagnosis result without considering the rotating speed of the induction motor will be discussed. This is nothing but the entire combinational data of all the four rotating speed. Fig. 12 and Fig. 13 shows the accuracy level of diagnosis for the combined data that is carried out for HF1, HF2, F1F2 and HF1F2. In this circumstance, the accuracy rate for HF1 and HF2 is comparatively high. But the accuracy level of F1F2 and HF1F2 is less. The reason behind this is other than the rotating speed 1780 min^{-1} of bearing with 0.5 mm and 1765 min^{-1} of bearing with 2 mm , the entire data of remaining rotating speed of the bearing with a hole of 0.5 mm and 2 mm is getting overlapped. This situation can be clearly understood from the Fig. 14. This is the reason that proper diagnosis could not be made by neglecting the rotating speed.

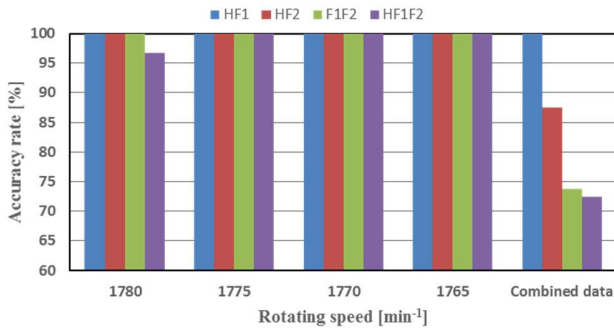


Fig. 12. Trial I diagnosis result.

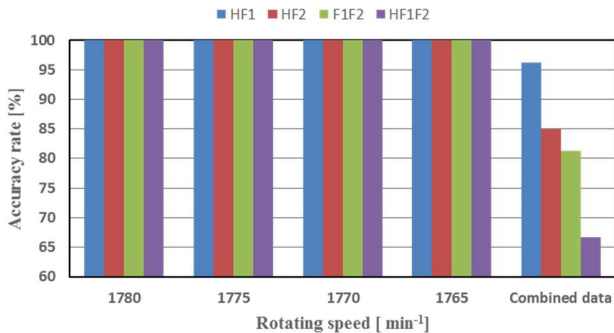


Fig. 13. Trial II diagnosis result.

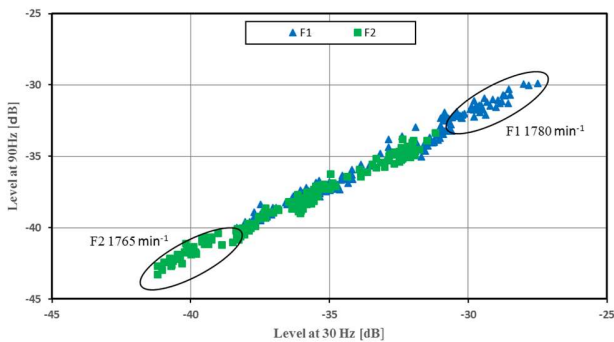


Fig. 14. Load current distribution of faulty 1 and faulty 2.

In the future, a method to improve the diagnosis and their accuracy level by neglecting the rotating speed of the induction motor will be investigated and the applicability of this proposed method to other kinds of the motor in the real world have to be studied and verified.

VI. CONCLUSION

In the present paper, through the FFT analysis, both healthy motor and the faulty motor can be differentiated under four bearing conditions (HF1, HF2, F1F2 and HF1F2). The entire analysis is done by considering the rotating speed of the induction motor. Their validity of the proposed method is verified by the experiments carried out in the laboratory.

Furthermore, as a supplementary work, a proper diagnosis is done for all the three types of bearing condition with the help of SVM. From the diagnosis result, it is clear that, for each individual rotating speed, the accuracy level is very high (almost 100%). This will be the cogency of the proposed system. Therefore, the proposed method has the following advantages:

- * High level of accuracy rate is achieved even for the slight failure in the bearing of the induction motor.
- * This method has a specific feature that the authors are able to distinguish and identify the bearing fault of 0.5 mm and 2 mm .
- * It can specify the condition of the bearing.
- * This method has an advantage of low cost and short data processing time.

On the other hand, the proposed methodology is not suitable for varying speed applications. In the future, an approach to improving the accuracy level for varying speed applications will be investigated by performing further analysis and experiments. In addition, future work should also evaluate this method for other bearing sizes, setup condition and other faulty locations like inner raceway effect, cage effect and ball effect. For a better assess of identifying the early fault detection, several experiments and more damage level should be included in the experimental setup.

ACKNOWLEDGMENT

The authors would gratefully acknowledge the contributions of Mr. Toshiki Matsumura and Mr. Keisuke Akahori during the experimental work and data analysis.

REFERENCES

- [1] A. Bellini, F. Filippetti, C. Tassoni, and G.A. Capolino, "Advances in diagnostic technique for induction machines," *IEEE Transactions on Industrial Electronics*, vol. 55, no. 12, pp. 4109-4126, Dec 2008.
- [2] S. Nandi, H.A. Toliyat and X. Li, "Condition monitoring and fault diagnosis of electrical motors-A review," *IEEE Transactions on Energy Conversion*, vol. 20, no. 4, pp. 719-729, Dec. 2005.
- [3] X. Jin, M.H. Azarian, C. Lau, L.L. Cheng, and M. Pecht, "Physics-of-failure analysis of cooling fan," in Proc. Prognost. Syst. Health Manage. Conf. Shenzhen, China, 2011, pp. 1-8.
- [4] "Report of large motor reliability survey of industrial and commercial installations, Part I," *IEEE Transactions on Industrial Applications*, vol. IA-21, no. 4, pp. 853-864, Jul. 1985.

- [5] W. Wang and M. Pecht, "Economic analysis of canary-based prognostics and health management," *IEEE Transactions on Industrial Electronics*, vol. 58, no. 7, pp. 3077-3089, Jul. 2011.
- [6] M. Cococcioni, B. Lazzerini, and S.L. Volpi, "Robust diagnosis of rolling element bearings based on classification techniques," *IEEE Transactions on Industrial Informatics*, vol. 9, no. 4, pp. 2256-2263, Nov. 2013.
- [7] M.D.Prieto, G.Cirincione, A.G. Espinosa, J. Ortega, and H. Henao, "Bearing fault detection by a novel condition-monitoring scheme based on statistical-time features and neural networks," *IEEE Transactions on Industrial Electronics*, vol. 60, no. 8, pp. 3398-3407, Aug. 2013.
- [8] R.B. Randall, *Vibration-based condition monitoring: Industrial, Aerospace and Automotive Application*. Chichester, U.K, Wiley, 2011, pp. 24-65, pp. 167-227.
- [9] W. Zhou, B. Lu, T. Habetler, and R. Harley, "Incipient bearing fault detection via motor stator current noise cancellation using wiener filter," *IEEE Transactions on Industry Applications*, vol. 45, no. 4, pp. 1309-1317, 2009.
- [10] M. Delgado, G. Cirincione, A. Garcia, J. Ortega, and H. Henao, "A novel condition monitoring scheme for bearing faults based on curvilinear component analysis and hierarchical neural networks," in *ICEM2012 - XXth International Conference on Electrical Machines*, 2012, pp. 2472-2478.
- [11] X. Jin, M. Zhao, T. Chow, and M. Pecht, "Motor bearing fault diagnosis using trace ratio linear discriminant analysis," *IEEE Transactions on Industrial Electronics*, vol. 61, no. 5, pp. 2441-2451, May 2014.
- [12] J. Rosero, L. Romeral, E. Rosero, and J. Urresty, "Fault detection in dynamic conditions by means of discrete wavelet decomposition for pmsm running under bearing damage," in *APEC 2009 - Twenty-Fourth Annual IEEE Applied Power Electronics Conference and Exposition*, 2009, pp. 951-956.
- [13] F. Immovilli, M. Cocconcelli, A. Bellini, and R. Rubini, "Detection of generalized-roughness bearing fault by spectral-kurtosis energy of vibration or current signals," *IEEE Transactions on Industrial Electronics*, vol. 56, no. 11, pp. 4710-4717, 2009.
- [14] A. Soualhi, G. Clerc, H. Razik, and A. Lebaroud, "Fault detection and diagnosis of induction motors based on hidden markov model," in *ICEM2012 - XXth International Conference on Electrical Machines*, 2012, pp. 1693-1699.
- [15] T. W. S. Chow and H. Z. Tan, "HOS-based nonparametric and parametric methodologies for machine fault detection," *IEEE Transactions on Industrial Electronics*, vol. 47, no. 5, pp. 1051-1059, Oct. 2000.
- [16] H. R. Martin and F. Honarvar, "Application of statistical moments to bearing failure detection," *Applied Acoustics*, vol. 44, no. 1, pp. 67-77, Jan. 1995.
- [17] R. B. W. Heng and M. J. M. Nor, "Statistical analysis of sound and vibration signals for monitoring rolling element bearing condition," *Applied Acoustics*, vol. 53, no. 1-3, pp. 211-226, Jan. 1998.
- [18] W. Zhou, T. G. Habetler, and R. G. Harley, "Bearing fault detection via stator current noise cancellation and statistical control," *IEEE Transactions on Industrial Electronics*, vol. 55, no. 12, pp. 4260-4269, Dec. 2008.
- [19] A. Soualhi, G. Clerc, and H. Razik, "Detection and diagnosis of faults in induction motor using an improved artificial ant clustering technique," *IEEE Transactions on Industrial Electronics*, vol. 60, no. 9, pp. 4053-4062, Sep. 2013.
- [20] F. Immovilli, A. Bellini, R. Rubini, and C. Tassoni, "Diagnosis of bearing faults in induction machines by vibration or current signals: A critical comparison," *IEEE Transactions on Industrial Applications*, vol. 46, no. 4, pp. 1350-1359, Jul./Aug. 2010.
- [21] X. Gong and W. Qiao, "Bearing fault diagnosis for direct-drive wind turbines via current-demodulated signals," *IEEE Transactions on Industrial Electronics*, vol. 60, no. 8, pp. 3419-3428, Aug. 2013.
- [22] Valeria C. M. N. Leite, J. G. B. da Silva, G. F. Cintra Veloso, L. E. B. da Silva, "Detection of Localized Bearing Faults in Induction Machines by Spectral Kurtosis and Envelope Analysis of Stator Current", *IEEE Transactions on Industrial Electronics*, vol. 62, No. 3, pp. 1855-1865, March 2015.
- [23] Christelle Piantsoy Mbo'o, Kay Hameyer, "Fault diagnosis of bearing damage by means of the linear discriminant analysis of stator current features from the frequency selection", *IEEE Transactions on Industrial Applications*, DOI. 10.1109/TIA.2016.2581139.
- [24] Jason R. Stack, Thomas G. Habetler, and Ronald G. Harley, "Fault-Signature Modeling and Detection of Inner-Race Bearing Faults", *IEEE Transactions on Industrial Applications*, vol. 42, No.1, pp. 61-67, Jan/Feb 2006.
- [25] S. Esakimuthu Pandarakone, C. Araki, Y. Mizuno and H. Nakamura, "Diagnosis method of mechanical failure in low voltage induction motor with the aid of support vector machine," in *ICEE 2016 - International Conference on Electrical Engineering*, 2016, Id. 90142.
- [26] J. R. Stack, R. G. Harley, and T. G. Habetler, "Fault classification and fault signature production for rolling element bearing in electric machines," *IEEE Transactions on Industrial Applications*, vol. 40, no. 3, pp. 735-739, May/Jun 2004.
- [27] M. S. Ballal, Z. J. Khan, H. M. Suryawanshi, and R. L. Sonolikar, "Adaptive neural fuzzy inference system for the detection of inter-turn insulation and bearing wear faults in induction motor," *IEEE Transactions on Industrial Electronics*, vol. 54, no. 1, pp. 250-258, Jan. 2007.
- [28] J. R. Stack, R. G. Harley, and T. G. Habetler, "An amplitude modulation detector for fault diagnosis in rolling element bearings," *IEEE Transactions on Industrial Electronics*, vol. 51, no. 5, pp. 1097-1102, May 2004.
- [29] S. Wu and T. W. S. Chow, "Induction machine fault detection using SOM-based RBF neural networks," *IEEE Transactions on Industrial Electronics*, vol. 51, no. 1, pp. 183-194, Jan. 2004.
- [30] B. Li, M. Chow, Y. Tipsuwan, and J. Hung, "Neural-network-based motor rolling bearing fault diagnosis," *IEEE Transactions on Industrial Electronics*, vol. 47, no. 5, pp. 1060-1069, Oct. 2000.
- [31] R. L. Schiltz, "Forcing frequency identification of rolling element bearings," *Sound and Vibration*, vol. 24, no. 5, pp. 16-19, May 1990.
- [32] K. B. Lipowits and T. R. Cundari, "Applications of Support Vector Machines in Chemistry", *Reviews in Computational Chemistry*, Vol. 23, Chap. 6, 2007.